The Plant Cell, Vol. 18, 3121–3131, November 2006, www.plantcell.org

Psb27, a Cyanobacterial Lipoprotein, Is Involved in the Repair Cycle of Photosystem II

Marc M. Nowaczyk,[a] Romano Hebeler,[b] Eberhard Schlodder,[c] Helmut E. Meyer,[b] Bettina Warscheid,[b] and Matthias Rögner[a,1]

[a] Plant Biochemistry, Ruhr-University Bochum, D-44780 Bochum, Germany
[b] Medical Proteom Center, Ruhr-University Bochum, D-44780 Bochum, Germany
[c] Max-Volmer-Lab for Biophysical Chemistry, Technical University Berlin, D-10623 Berlin, Germany

Photosystem II (PSII) performs one of the key reactions on our planet: the light-driven oxidation of water. This fundamental but very complex process requires PSII to act in a highly coordinated fashion. Despite detailed structural information on the fully assembled PSII complex, the dynamic aspects of formation, processing, turnover, and degradation of PSII with at least 19 subunits and various cofactors are still not fully understood. Transient complexes are especially difficult to characterize due to low abundance, potential heterogeneity, and instability. Here, we show that Psb27 is involved in the assembly of the water-splitting site of PSII and in the turnover of the complex. Psb27 is a bacterial lipoprotein with a specific lipid modification as shown by matrix-assisted laser-desorption ionization time of flight mass spectrometry. The combination of HPLC purification of four different PSII subcomplexes and ^{15}N pulse label experiments revealed that lipoprotein Psb27 is part of a preassembled PSII subcomplex that represents a distinct intermediate in the repair cycle of PSII.

INTRODUCTION

The photosynthetic electron transfer chain of cyanobacteria, eukaryotic algae, and vascular plants is located in a specialized membrane system, the thylakoids, and mediated by the integral membrane protein complexes photosystem II (PSII), cytochrome b_6f complex, and photosystem I (PSI). Electron transfer is initiated in the PSII complex by light-induced charge separation at the central chlorophyll redox center P_{680}, and electrons are transferred to the quinone B binding site via a short internal redox chain (Diner and Rappaport, 2002). P_{680}^+ is reduced by electrons provided by the water-splitting system at the luminal side of PSII, which contains four manganese ions and one calcium ion (Rutherford and Boussac, 2004).

Structural studies have provided a detailed static view of PSII (Zouni et al., 2001; Kamiya and Shen, 2003; Ferreira et al., 2004; Loll et al., 2005). The monomeric complex contains at least 19 protein subunits, seven carotenoids, two hemes, one nonheme iron, two phaeophytins, and 36 chlorophylls as deduced from x-ray data (Ferreira et al., 2004). The core center proteins D1 and D2 each contain five transmembrane helices and bind most of the redox centers of the intrinsic electron transfer chain. Light energy is transferred to the core by the intrinsic antenna proteins CP43 and CP47, which bind most of the chlorophyll molecules in the complex. The water-splitting system at the luminal side is shielded in cyanobacteria by the extrinsic proteins PsbO, PsbV, and PsbU (Seidler, 1996). Several small subunits with, in most cases, unknown function are structural constituents of the complex (Shi and Schroder, 2004).

Although structural information is provided in great detail, only little is known about the dynamic aspects of the PSII life cycle, including transient complexes and factors involved in the biogenesis, maintenance, repair, and degradation of the complex (Nickelsen et al., 2006). The first step of biogenesis includes the integration of the transmembrane helices and central redox centers into the lipid phase followed by the formation of an initial PSII precomplex built by D1, D2, cytochrome b559, and PsbI (Komenda et al., 2004; Aro et al., 2005). This process could happen spontaneously or guided by factors like HCF136, which was shown to interact specifically with a PSII precomplex (Plucken et al., 2002). The precomplex is transformed into an active complex by attachment of the intrinsic antenna proteins CP43/CP47, incorporation of several small subunits, and assembly of the water-splitting system. Fine tuning of the latter process is provided by C-terminal processing of D1, a prerequisite for the formation and photoactivation of the Mn cluster and the assembly of the extrinsic proteins. This complex procedure is initiated by the action of CtpA, the D1-processing peptidase, which cleaves the D1 C-terminal extension (Anbudurai et al., 1994). Other factors like PratA (Klinkert et al., 2004) are involved in this process. Finally, the active monomeric functional unit is transformed into the most prominent dimeric complex. Protein factors like PsbP and PsbQ in cyanobacteria (Thornton et al., 2004; Summerfield et al., 2005a, 2005b) or Psb29 in cyanobacteria and vascular plants (Keren et al., 2005) have been shown to be necessary for optimal function and maintenance of assembled PSII complexes. Others like the iron stress–induced protein

[1] To whom correspondence should be addressed. E-mail matthias.roegner@rub.de; fax 49-234-3214322.
The author responsible for distribution of materials integral to the findings presented in this article in accordance with the policy described in the Instructions for Authors (www.plantcell.org) is: Matthias Rögner (matthias.roegner@rub.de).
www.plantcell.org/cgi/doi/10.1105/tpc.106.042671

IdiA (Michel et al., 1996) play a role in protection of the complex under certain stress conditions.

Photosynthetic water splitting is inevitable coupled with the formation of reactive oxygen species followed by photooxidative damage of protein subunits even under low light conditions (Anderson et al., 1997; Keren et al., 2005). Therefore, the D1 protein, which is the major target for photoinhibition, and other subunits are continuously replaced in a complex process called the PSII repair cycle (Aro et al., 2005). While some steps of this cycle are identical to the de novo biogenesis of the complex, others are specific and involve special protein factors. Much effort has been made to identify the proteases responsible for the degradation of the D1 subunit, and it seems that at least in cyanobacteria, the FtsH protease plays the major role in this process (Kamata et al., 2005; Nixon et al., 2005; Komenda et al., 2006). Interestingly, at least some vascular plants exhibit a PSII subfraction with D1 being palmitoylated (Mattoo and Edelman, 1987; Gomez et al., 2002), but the function of this lipid modification is still unclear.

Another intriguing and still unresolved question is the spatial organization of the different parts of the PSII life cycle. The idea of specialized regions for the biogenesis of photosystems was strongly supported by the detection of preassembled PSI and PSII complexes in the cytoplasmic membrane of cyanobacteria (Zak et al., 2001); however, it is still unknown how the two membrane systems are interconnected and how lipid and protein transfer occurs between them.

Here, we report about four different transient complexes that represent particular steps in the life cycle of PSII. Among them, the PSII/Psb27 complex is of special interest. It was shown by the combination of intact mass tag analysis, introduced by Gomez et al. (2003), and enzymatic cleavage that the Psb27 subunit is specifically lipid modified. Moreover, the ^{15}N pulse label approach presented in this study allows analysis of both synthesis and degradation of individual PSII subunits, enabling monitoring of the dynamics of the PSII subcomplexes and especially the ability to distinguish between complexes involved in biogenesis or repair of PSII.

RESULTS

Combination of Ni-Chelating and Ion Exchange Chromatography Enables the Isolation of Four Different PSII Subcomplexes

For the efficient isolation of reaction centers from *Thermosynechococcus elongatus*, 10 His residues were fused to the C terminus of the PSII subunit CP43. *His*-tagged PSII complexes were purified via Ni chelate affinity chromatography (Figure 1) followed by continuous bed ion exchange chromatography (IEC), which resulted in the isolation of four different PSII subfractions (Figure 2A). Applying HPLC size exclusion chromatography and native PAGE (Figure 2B), we could identify two characteristic monomeric complexes, termed $PSII_{M(low)}$ and $PSII_{M(high)}$ (fractions 1 and 2), and two distinct dimeric complexes, termed $PSII_{D(high)}$ and $PSII_{D(low)}$ (fractions 3 and 4). Activity measurements on the purified subcomplexes revealed as highest activity

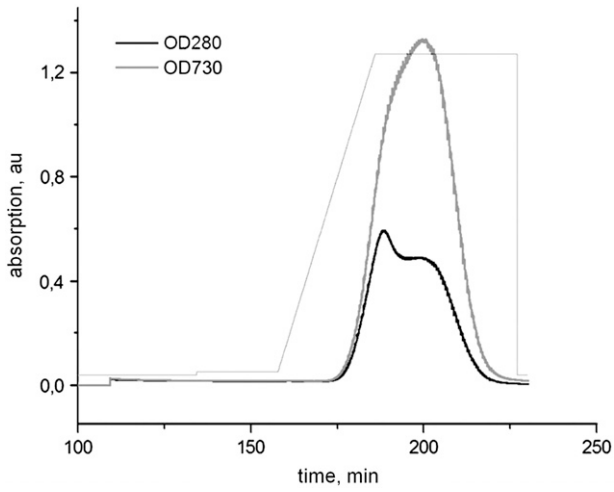

Figure 1. Purification of *His*-Tagged PSII Complexes.

His-tagged PSII complexes were eluted with a linear gradient of 1 to 100 mM histidine (light-gray line) from a Ni-NTA sepharose column. The elution profile is shown at 280 nm (arbitrary units [au]; black line) and at 730 nm (dark-gray line). For details, see Methods.

4790 μmol O_2 (mg Chl)$^{-1}$ h^{-1} for $PSII_{D(high)}$ (fraction 3), >50% lower activity of 2070 μmol O_2 [mg Chl]$^{-1}$ h^{-1} for $PSII_{D(low)}$ (fraction 4), a moderate activity of 2920 μmol O_2 [mg Chl]$^{-1}$ h^{-1} for $PSII_{M(high)}$ (fraction 2), and a marginal activity of 210 μmol O_2 [mg Chl]$^{-1}$ h^{-1} for $PSII_{M(low)}$ (fraction 1).

Transient Absorption Spectroscopy Reveals Light-Induced Charge Separation in the four PSII Subcomplexes

$P680^+Q_A^-$- $P680Q_A$ (Q_A for primary electron accepting plastoquinone of PSII) absorption difference spectra of the inactive $PSII_{M(low)}$ subcomplex and the active PSII subcomplexes did not show significant differences, indicating the integrity of the reaction centers (Figure 3). However, an increased number of chlorophylls per reduced Q_A could be determined for $PSII_{M(low)}$, which reflects a larger antenna size in comparison with the active PSII subfractions (Table 1) and may be either due to an impaired assembly in vivo or a loss of Q_A.

SDS-PAGE Analysis Shows the Presence of Psb27 in $PSII_{M(low)}$

Figure 2C shows the SDS-PAGE gels of the four different PSII subpopulations. The polypeptide patterns of active $PSII_{M(high)}$ and highly active $PSII_{D(high)}$ and $PSII_{D(low)}$ are in good agreement with previous results obtained for a PSII preparation from *T. elongatus* (Kuhl et al., 2000). Distinct bands of the major PSII subunits CP47, CP43 (with a mass shift due to the *His*-tag), D1, D2, and the extrinsic proteins PsbO, PsbV, and PsbU were consistently observed for all three subcomplexes after gel staining with Coomassie blue. In addition, uniform band patterns were observed in the low molecular mass region for $PSII_{M(high)}$, $PSII_{D(high)}$, and $PSII_{D(low)}$. By contrast, SDS-PAGE analysis of inactive $PSII_{M(low)}$ revealed the absence of the three extrinsic

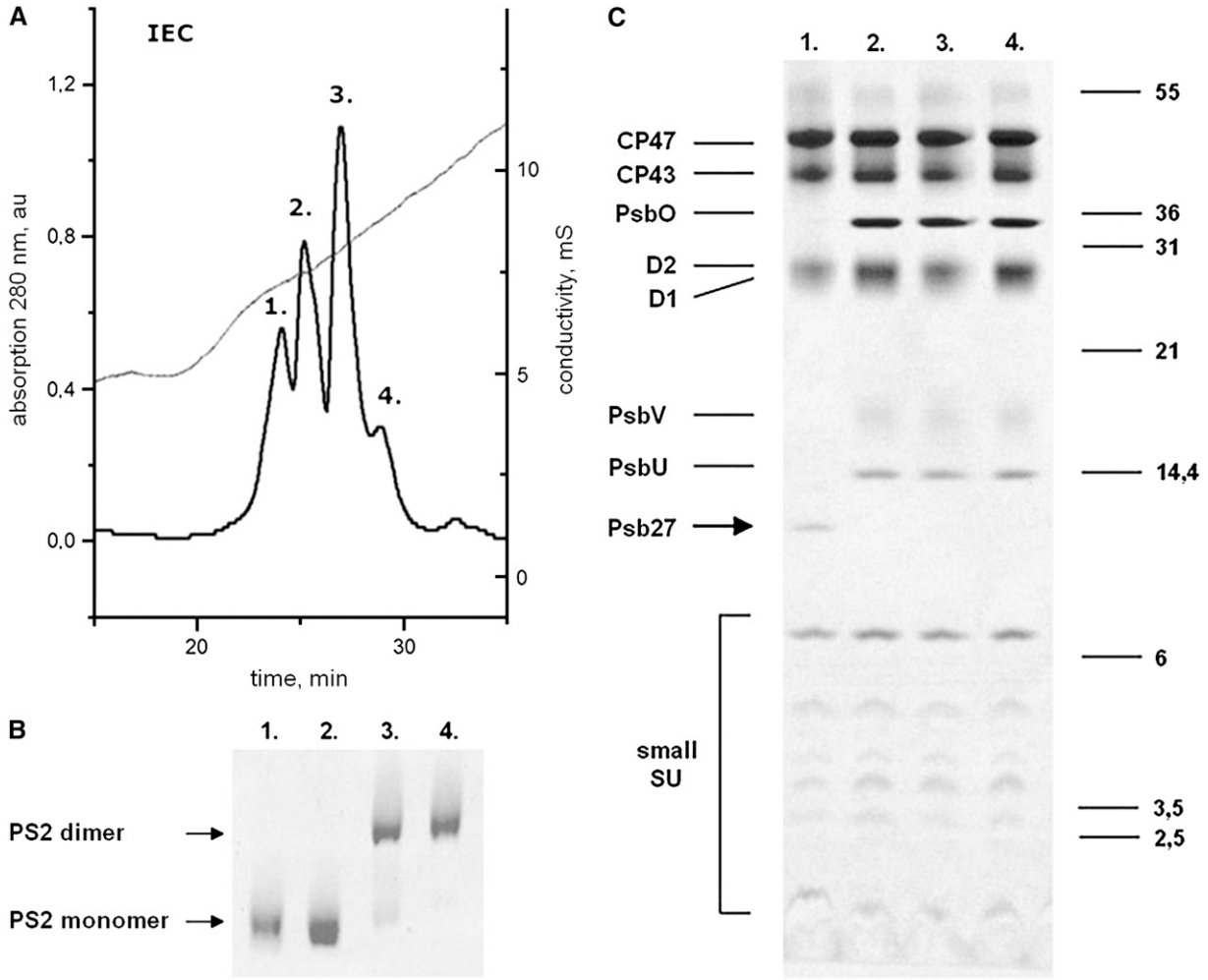

Figure 2. Purification and Characterization of *His*-Tagged PSII Complexes.

(A) Elution profile from an UNO Q6 ion exchange column (Bio-Rad) of prepurified *His*-tagged PSII complexes. Individual PSII subfractions: 1, $PSII_{M(low)}$; 2, $PSII_{M(high)}$; 3, $PSII_{D(high)}$; 4, $PSII_{D(low)}$.

(B) Monomer/dimer analysis of PSII subcomplexes by native-PAGE.

(C) SDS-PAGE profiles showing the differences in subunit (SU) composition of the four IEC subfractions. Each lane was loaded with 2 μg Chl. For details, see Methods.

subunits PsbO, PsbV, and PsbU. Instead, a novel component of ~11 kD was instead observed in the low molecular mass range, which could be identified as Psb27 (Kashino et al., 2002) via mass spectrometric sequence analysis. Interestingly, no manganese could be detected in the $PSII_{M(low)}$ subcomplex (Table 1), although the C terminus of its D1 subunit seems to be already processed (Figure 4).

Psb27 Is Shown to Be a Bacterial Lipoprotein

Hydropathy plots and sequence analysis with TMHMM (Krogh et al., 2001) predict that Psb27 is a soluble protein that lacks membrane-spanning helices. To confirm this prediction, $PSII_{M(low)}$ complexes were exposed to a variety of different treatments, as summarized in Table 2. Among them, washing with 1 M $CaCl_2$ (Ono and Inoue, 1983) or 1 M Tris, pH 8.8 (Yamamoto and Ke, 1981), represents well-established procedures to separate the extrinsic, lumen-exposed proteins PsbO, PsbV, and PsbU from PSII. Since all selected washing procedures failed to release Psb27 from $PSII_{M(low)}$ (Table 2), we propose a strong hydrophobic interaction between Psb27 and the PSII core center. In contrast with a $CaCl_2$-washed PSII complex, binding of the extrinsic protein PsbO, PsbU, or PsbV to the $PSII_{M(low)}$ complex was not observed in reconstitution assays (Figure 5). This suggests that the lumen-exposed PSII domain, which is required for binding of extrinsic PSII proteins, is effectively blocked by Psb27. A lumen-exposed localization of Psb27 is also consistent with its bacterial signal sequence as predicted by the SignalP algorithm (Bendtsen et al., 2004). Such a motif is commonly known to direct subunits across the membrane into the luminal space. A detailed

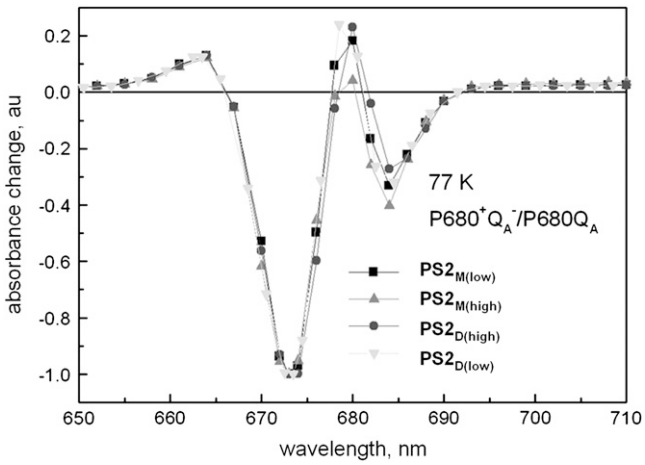

Figure 3. $P680^{+}Q_A^{-}$ - $P680Q_A$ Difference Spectra of PSII Core Complexes from $PSII_{M(low)}$, $PSII_{M(high)}$, $PSII_{D(high)}$, and $PSII_{D(low)}$.

The spectra have been recorded at 77K and are normalized to the bleaching minimum. While the main bleaching at 674 nm could be assigned to the oxidation of P680, the absorbance increase at 680 nm and the absorbance decrease at 684 nm have been assigned to an electrochromic blue shift of the Q_Y absorption band of the accessory chlorophyll (Diner et al., 2001). Triangles, $PSII_{M(low)}$; squares, $PSII_{M(high)}$; circles, $PSII_{D(high)}$; inverse triangles, $PSII_{D(low)}$.

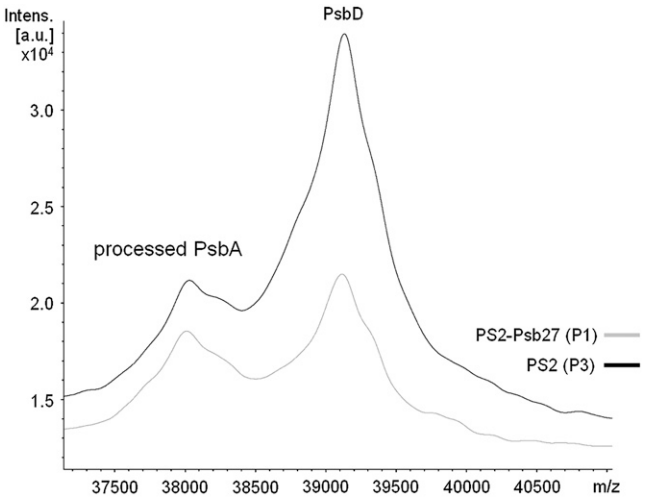

Figure 4. Processing of the D1 Protein.

Intact $PSII_{M(low)}$ (gray) and $PSII_{D(high)}$ (black) complexes were analyzed in the mass-to-charge (*m/z*) range between 37.000 and 41.000 by MALDI-TOF. The assignment of the peaks is based on the calculated masses for unprocessed D1 (SwissProt primary accession number P0A444; molecular mass 39,605 D), processed D1 (38,109 D), and D2 (Q8CM25; 39,230 D).

sequence analysis of Psb27 from various cyanobacteria (Figure 6) also showed a highly conserved Cys residue in the N-terminal leader sequence. As predicted by the online servers DOLOP (Madan Babu and Sankaran, 2002) and LIPOP (Juncker et al., 2003), this Cys residue is combined with a sequence motif called lipobox, which is unique for bacterial lipoproteins (Figure 6). Proteomics analysis of the thylakoid lumen of *Arabidopsis thaliana* revealed the presence of a Psb27 homologue (Peltier et al., 2002); however, in contrast with cyanobacteria, eukaryotes are lacking both the lipobox sequence motif and the maturation system consisting of a diacylglycerol transferase, a lipoprotein signal peptidase, and an apolipoprotein *N*-acyltransferase, which are required for the specific lipid modification.

To confirm the presence of lipid-modified Psb27 in the $PSII_{M(low)}$ complex as purified in this work, the isolated intact subcomplex was subjected to enzymatic cleavage with unspecific lipase. Intact mass tag analysis (Whitelegge et al., 1997, 1998; Gomez et al., 2002) was used to monitor the cleavage of the lipid modification. Spectra of Psb27 present in $PSII_{M(low)}$ were obtained in situ after various incubation times with Lipolase by quadrupole-time-of-flight mass spectrometry (qTOF-MS) following matrix-assisted laser-desorption ionization (MALDI).

Figure 7 shows sections of MALDI-qTOF-MS spectra from the $PSII_{M(low)}$ subcomplex in the *m/z* range of 12 to 14 kD before and after treatment with Lipolase. Intact mass tags of photosynthetic proteins were acquired with high mass accuracy (e.g., ~100 ppm at 13.5 kD), allowing the reliable assignment of structural components of the $PSII_{M(low)}$ subcomplex. The peak observed at *m/z* 13518.1 in the MALDI spectrum of the intact $PSII_{M(low)}$ subcomplex could be assigned to Psb27 posttranslationally modified by three fatty acid residues ($Psb27_{nat}$) as shown in Figure 7 (inset a). For further confirmation, enzymatic cleavage of $PSII_{M(low)}$/Psb27 subcomplexes by Lipolase was allowed to proceed for 5 and 30 min, respectively. After 5 min, a distinct peak at *m/z* 13252.3 appeared in the MALDI spectrum, which corresponds to the cleavage of octadecanoic acid from $Psb27_{nat}$, resulting in $Psb27_{P1}$ (Figure 7, inset b). A prolonged Lipolase treatment of 30 min resulted in an additional peak at *m/z* 13013.2; this molecular mass is consistent in molecular mass with $Psb27_{P2}$ (Figure 7, inset c) (i.e., an enzymatic cleavage of octadecanoic acid and hexadecanoic acid residues from $Psb27_{nat}$). $Psb27_{P2}$

Table 1. Characterization of the PSII Subpopulations

IEC Fraction	1	2	3	4
Mon./dim.	Mon.	Mon.	Dim.	Dim.
Rel. amount	18%	22%	43%	17%
μmol O_2 (mg Chl)$^{-1}$ h^{-1}	210	2925	4788	2069
Chl per reduced Q_A	64	42	38	42
Mn	−	+	+	+

Mon., monomer; Dim., dimer; Rel. amount, relative amount; oxygen evolving activity, μmol O_2 (mg Chl)$^{-1}$ h^{-1}.

Table 2. Various Treatments to Probe for the Dissection of the $PSII_{M(low)}$-Psb27 Complex

	NaCl	$CaCl_2$	Urea	Tris	$NaCO_3$	OGP[a]
Final concentration	1 M	1 M	2.6 M	1 M	100 mM	60 mM
pH	6.5	6.5	6.5	8.0	11	6.5
Selective release of Psb27	–	–	–	–	–	–

[a] OGP, *n*-octyl-β-D-glucopyranoside.

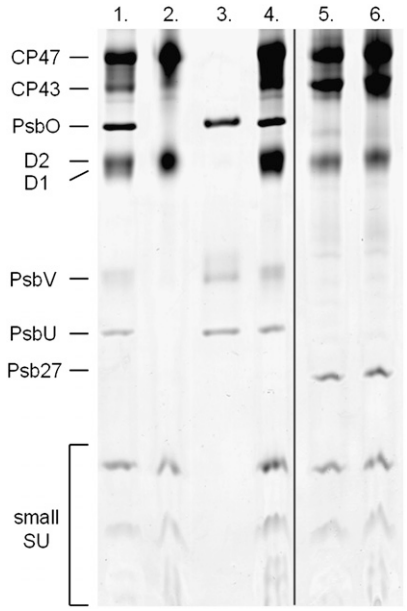

Figure 5. SDS-PAGE Analysis of PSII/Psb27 Complexes Reconstituted with the Extrinsic PSII Proteins PsbO, PsbV, and PsbU.

Lane 1, $PSII_{D(high)}$; lane 2, $PSII_{D(high)}$ after treatment with 1 M $CaCl_2$ to remove the extrinsic proteins PsbO, PsbV, and PsbU; lane 3, released extrinsic proteins; lane 4, $PSII_{D(high)}$ after treatment with 1 M $CaCl_2$ and reconstitution with the released extrinsic proteins; lane 5, $PSII_{M(low)}$-Psb27 complex; lane 6, $PSII_{M(low)}$-Psb27 after reconstitution with PsbO, PsbV, and PsbU.

still contains the residual glycerol modification and an amide-linked hexadecanoic acid residue (C16:0).

^{15}N Pulse Label Experiments Indicate Involvement of the PSII/Psb27 Complex in the Repair Process of PSII

Time-dependent distribution of the PSII subcomplexes was analyzed by pulse label experiments using ^{15}N-enriched media (98% purity) combined with MALDI-TOF/TOF-MS analyses (Figure 8). During the mid-log growth phase, the nitrogen source was shifted from ^{14}N to ^{15}N, and $PSII_{M(low)}$ and $PSII_{D(high)}$ subcomplexes were isolated at various times after the ^{15}N pulse. Isolated $PSII_{M(low)}$ and $PSII_{D(high)}$ were separated by SDS-PAGE and ^{15}N incorporation into the D1 subunit of the respective complex was analyzed by MALDI-TOF analysis of the corresponding tryptic peptide mixtures. For $PSII_{M(low)}$, an ~25% ^{15}N incorporation could be observed 3 h after the ^{15}N pulse, while for $PSII_{D(high)}$, no incorporation could be detected (Figure 8, $PSII_{M(low)}$/3 h and $PSII_{D(high)}$/3 h). Accordingly, the amount of incorporated ^{15}N atoms was distinctly higher (~75%) in $PSII_{M(low)}$ than in the active PSII dimer (~45%) 10 h after the pulse (Figure 8, $PSII_{M(low)}$/10 h and $PSII_{D(high)}$/10 h).

To further analyze the role of the $PSII_{M(low)}$ subcomplex in the de novo biogenesis or repair of PSII, the incorporation of ^{15}N was also monitored for different PSII subunits 24 h after the ^{15}N pulse (Figure 9). It is obvious that the D1 subunit exhibits the highest amount of newly synthesized protein (~96%), whereas all other analyzed subunits clearly show a higher proportion of old (^{15}N-free) protein. In conclusion, the $PSII_{M(low)}$ complex seems mainly determined by the repair cycle of D1, as in case of a de novo biogenesis of the whole complex, a more or less uniform ^{15}N incorporation into all involved subunits would be expected. On the other hand, our data do not exclude the de novo biogenesis for a minor subfraction of $PSII_{M(low)}$. Our results also show that, interestingly, the ^{15}N incorporation rate differs between the other analyzed subunits. Approximately 75% of newly synthesized protein for CP43 and ~65% for the D2 subunit indicate a higher turnover of these subunits compared to CP47 (~45%) and PsbE (~35%). With its minimal synthesis rate ($t1/2 = 37$ h), the latter may be regarded as a kind of internal standard, as it corresponds roughly to the doubling time of the cells (~35h) under the experimental conditions.

DISCUSSION

In conclusion, these results provide strong evidence that Psb27 plays a role in the biogenesis of the water-splitting site that is most critical for the function of PSII and especially for the repair of damaged PSII complexes. The $PSII_{M(low)}$-Psb27 complex represents an intermediate state in which the integral membrane part is fully assembled and capable of primary charge separation and electron transfer. These results are in agreement with data from Roose and Pakrasi (2004) showing that a Δ*ctpA*- strain of *Synechocystis* is not able to assemble functional PSII and accumulates instead a preassembled $PSII_{M(low)}$-Psb27 complex, suggesting a role for Psb27 in the C-terminal processing of D1. In combination with the growing evidence that a partial assembly of the PSII core complex, with a processed D1 subunit (however,

Psb27

Thermosynechococcus elongatus	--------MKRFWAMVCALFLSVSLLLTSCA-NVPTGLTGNFREDTLALI
Synechocystis PCC6803	-----MSFLKNQLSRLLALILVVAIGLTAC--DSGTGLTGNYSQDTLTVI
Synechococcus WH8102	MISALARLIQQLSRAAVALVLGLCLLLTACSGDAEARLTGDYVEDTIAVA
Synechococcus elongatus PCC794	--------MARPLARLFAIVLVAVIGLTACTGGGDSAISGNYRQDTLAVV
Anabaena variabilis	------MLMKRYWSRLLALVLVVAIGLVGC--GSPDSLTGDYRQDTLAVV
Nostoc punctiforme PCC73102	------MHMKRYWSRLLALVLVVSIGLMGCT-GSPDSLTGDYRQDTLAVV
Crocosphaera watsonii WH8501	------MFFKSALSRILALVLVAVVTLTGCG-NSSSGLSGNYSEDTLAVI
Trichodesmium erythraeum	--------MKSFISRLLALVLVCAIGLMGC--SNPSTLSGNYSEDTLSLI

Figure 6. Signal Peptides of Psb27 from Different Species.

Characteristic features of the signal peptides are labeled as follows: horizontal bar, region of hydrophobic and uncharged residues; boxed region, Lipobox motif with the invariant Cys residue (+1).

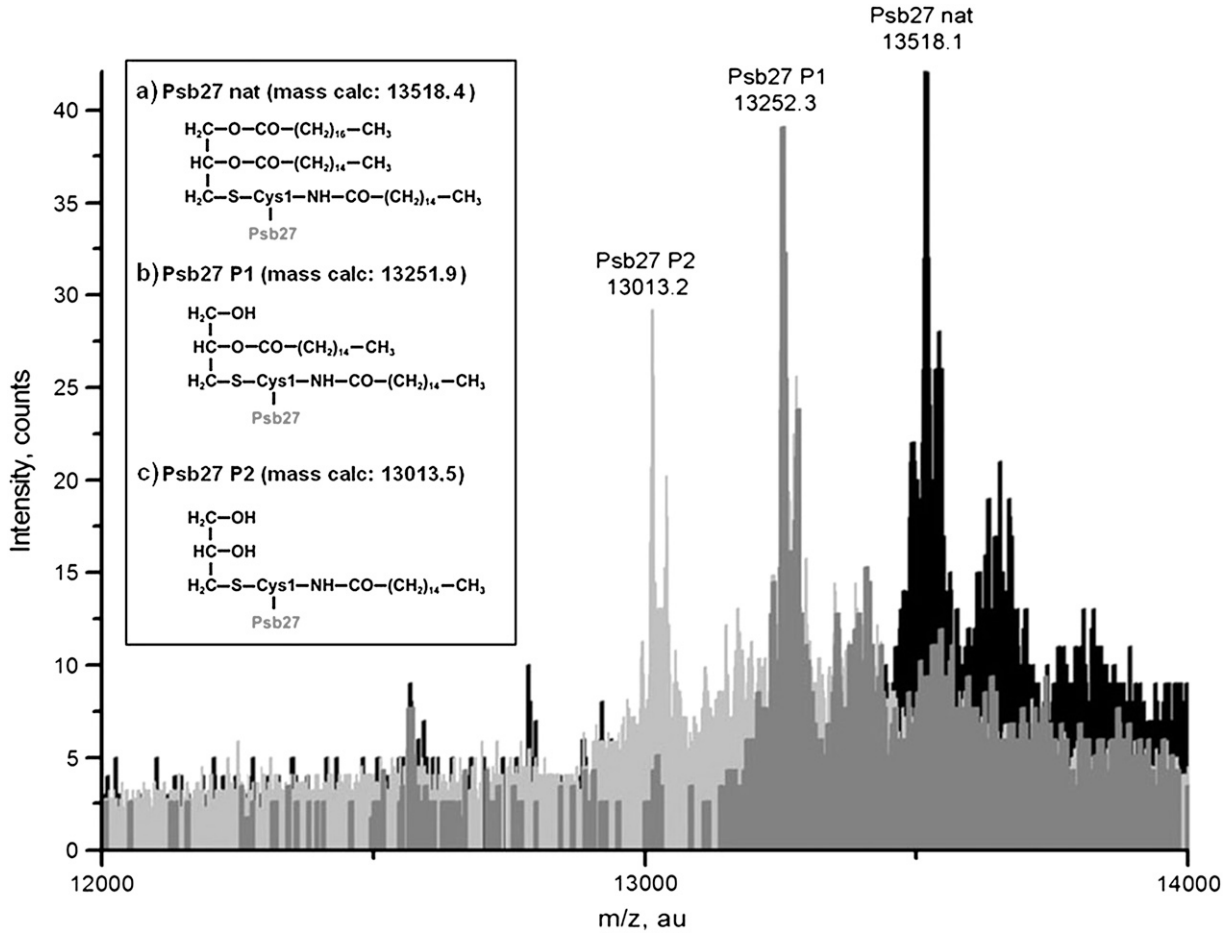

Figure 7. MS Analysis of Psb27.

Intact $PSII_{M(low)}$ complexes were analyzed by MALDI-TOF with or without Lipolase treatment to determine the accurate mass of Psb27 (SwissProt primary accession number Q8DG60) and to probe the prediction of the posttranslational lipid modification. Masses in a *m/z* range of 12,000 to 14,000 were detected before (native Psb27; black) and after 5 min (P1; grey) or 30 min (P2; light gray) of Lipolase treatment (for details, see Methods). The inset shows the model and the calculated (total) mass of the best-suited Psb27 lipid modification based on the masses determined at each stage.

without water splitting), occurs in the cyanobacterial plasma membrane (Zak et al., 2001; Klinkert et al., 2004; Keren et al., 2005), the $PSII_{M(low)}$-Psb27 complex could also represent a transit complex for the transfer from the cytoplasmic to the thylakoid membrane. Physiologically, such an arrested intermediate could be of vital importance, as a premature start of water splitting could easily lead to the production of dangerous reactive oxygen species or maybe an easy target for destruction. However, up to now, Psb27 was not shown to be associated with the plasma membrane of cyanobacteria, and, interestingly, *Gloeobacter violaceus*, a primitive cyanobacterium that lacks a separate thylakoid membrane system, exhibits no Psb27 homologue. On the other hand, there is evidence that the $PSII_{M(low)}$-Psb27 complex of our study should be located in the thylakoid membrane: It was isolated via a *His*-Tag attached to subunit CP43, which was reported to be absent in the cytoplasmic membrane (Zak et al., 2001). While we cannot exclude a general role of the $PSII_{M(low)}$-Psb27 complex in the biogenesis of PSII, our data strongly suggest that the $PSII_{M(low)}$-Psb27 complex is an intermediate in the PSII repair cycle (as reviewed in Aro et al., 2005), which continuously replaces the D1 subunit (and maybe others; Figure 10). Such a model is consistent with data showing impairment of PSII recovery after photoinhibition in a Psb27 knockout line of *Arabidopsis* (Chen et al., 2006). The association of Psb27 with dynamic processes of PSII and the fact that many more lipoproteins with still unknown function are predicted from genomic data might reveal a more general role of lipoproteins in photosynthesis and elsewhere. This would be in line with examples for lipidated proteins (Mattoo and Edelman, 1987; Gomez et al., 2002) and with the general importance of lipid–protein interactions (Fyfe et al., 2005) in photosynthesis.

Especially for membrane proteins, this report shows the potential of HPLC purification in combination with state-of-the-art MS for the characterization of transient complexes. Such

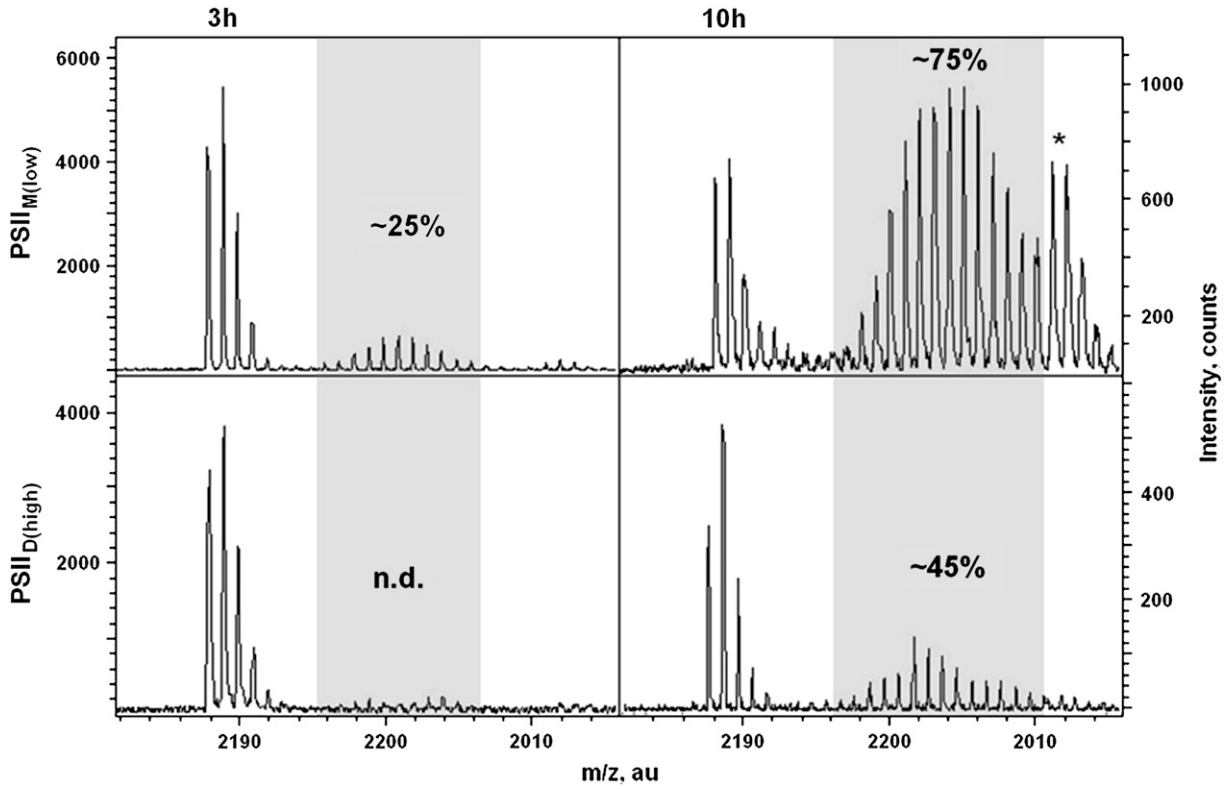

Figure 8. Analysis of ^{15}N Incorporation into the D1 Subunit of PSII.

T. elongatus cells, grown in a medium with the natural nitrogen isotope ^{14}N (99.6%), were exposed to a medium highly enriched in the stable isotope ^{15}N (>98%) at the mid-log growth phase. Cells were harvested 3 and 10 h after the ^{15}N pulse, followed by an immediate preparation of PSII subcomplexes. Subunits of each PSII subcomplex were separated by SDS-PAGE, and the D1 subunit was subjected to tryptic digestion and MALDI-TOF analysis (for details, see Methods). The top row (P1) shows the incorporation of ^{15}N into a peptide (calculated mass 2188.3 D) from the D1 subunit (SwissProt primary accession number P0A444) of the $PSII_{M(low)}$-Psb27 complex 3 h (left column) and 10 h (right column) after the pulse. Spectra of the bottom row (P3) show the corresponding peptide from the D1 subunit of the $PSII_{D(high)}$ complex. The percentage of newly synthesized D1 protein was calculated from the spectra. A peak corresponding to an autocatalytic product of trypsin is marked by an asterisk.

a combined approach may contribute to better understanding of dynamic processes of membrane protein complexes with transient intermediates of limited stability and low abundance.

METHODS

Preparation of *His*-Tagged PSII and Analytical Size Exclusion Chromatography

His-tagged PSII complexes (10× His fused to the C terminus of the CP43 subunit) were isolated from cells that had been grown under normal light conditions (~30 μE) and that had been harvested in the exponential growth phase. Cells were otherwise processed as previously reported by Kuhl et al. (2000). For the ^{15}N pulse label experiments, $NaNO_3$ was substituted by 5 mM $^{15}NH_4Cl$ in the media. Thylakoid membranes were solubilized in 20 mM MES, pH 6.5, 10 mM $CaCl_2$, 10 mM $MgCl_2$, 1.2% *n*-dodecyl-β,D-maltoside (β-DM; Biomol), and 0.5% Na-cholate (Dojindo) at a chlorophyll concentration of 1 mg/mL. After centrifugation at 45,000*g* for 90 min at 4°C, the supernatant was loaded onto a chelating sepharose fast flow column (Pharmacia) that was equilibrated with buffer (20 mM MES, pH 6.5, 10 mM $CaCl_2$, 10 mM $MgCl_2$, 300 mM NaCl, 500 mM mannitol, 0.03% β-DM, and 1 mM histidine). The column was then washed with 4 volumes of equilibration buffer at a flow rate of 2 mL min^{-1}. PSII complexes were eluted by a linear gradient of 1 to 100 mM histidine. To separate different PSII subfractions by IEC, the resulting protein solution was dialyzed against buffer (20 mM MES, pH 6.5, 20 mM $CaCl_2$, 20 mM $MgCl_2$, 0.5 M mannitol, and 0.03% β-DM) overnight and loaded onto a UNO Q6 column (Bio-Rad) as previously reported by Kuhl et al. (2000). The oligomerization status of PSII was monitored by analytical size exclusion chromatography using a TSK-gel 4000 SW_{XL} column (TosoHaas) in a Waters HPLC system (for details, see Kuhl et al., 2000).

PSII Activity Measurements, SDS-PAGE, and Native PAGE

Light-induced rates of oxygen evolution were determined at 25°C using a home-made setup, which consists of a thermostated 1-mL cuvette, a highly sensitive oxygen sensor (Presens), and continuous, saturating red light (12,000 μE) from a 250-W cold light source (Schott). PSII complexes were suspended in buffer (20 mM MES, pH 6.5, 30 mM $CaCl_2$, 10 mM

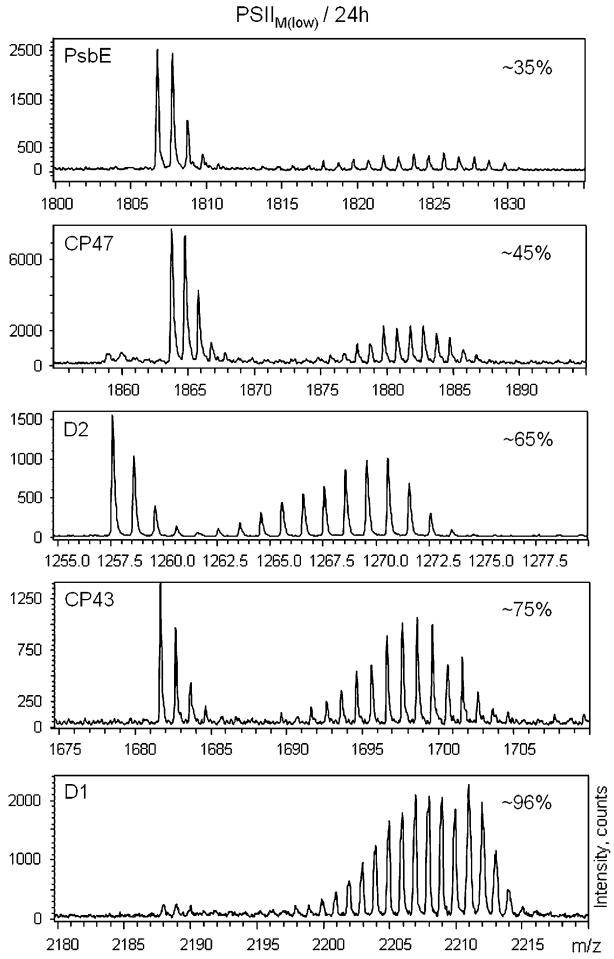

Figure 9. Analysis of ^{15}N Incorporation into Different Subunits of PSII$_{M(low)}$.

T. elongatus cells were harvested 24 h after the ^{15}N pulse, followed by preparation of PSII$_{M(low)}$ and SDS-PAGE analysis. Several subunits were subjected to tryptic digestion and analyzed by MALDI-TOF. The incorporation of ^{15}N was followed into peptides of PsbE (SwissProt primary accession number Q8DIP0; molecular mass 1806.9 *m/z*), D1 (P0A444; 2188.3 *m/z*), D2 (Q8CM25; 1257.3 *m/z*), CP43 (Q8DIF8; 1681.7 *m/z*), and CP47 (Q8DIQ1; 1864.0 *m/z*), and the amount of newly synthesized protein was calculated.

$MgCl_2$, 1 M betaine, 0.03% β-DM) at a concentration of ~2 to 5 μg Chl mL^{-1}. Ferricyanide and 2,6-dichloro-*p*-benzoquinone (at 1 mM each) were used as artificial electron acceptors. Polypeptide composition of isolated PSII complexes was analyzed by denaturing SDS-PAGE with a 12% polyacrylamide gel and 6 M urea according to Schägger and von Jagow (1987). Samples were solubilized in sample buffer with 1% SDS and 5% β-mercaptoethanol prior to electrophoresis. Nondenaturing Deriphat PAGE analysis was performed according to Peter and Thornber (1991) with the following modifications. Samples were sedimented in a centrifuge and resuspended in 25 mM Tris, 200 mM glycine, 25% glycerol, and β-DM to reach final concentrations of 1 mg/mL chlorophyll and 1% β-DM. After incubation at 4°C for 15 min, samples were centrifuged for 5 min at 13,000*g* and loaded onto a 4 to 6% acrylamide gradient gel (10 × 10 × 0.1 cm; 25 mM Tris, 200 mM glycine, and 0.3% Deriphat), overlaid by a 3% acrylamide stacking gel (12.5 mM Tris/HCl, pH 6.6, and 100 mM glycine). The acrylamide:bisacrylamide ratio was 37.5:1. Reservoir buffer contained 12.5 mM Tris and 100 mM glycine, the upper one including 0.2% Deriphat. Electrophoresis was carried out at 120 V and at 11°C for 14 h.

PSII Reconstitution and Dissection Experiments

Purified PSII His complexes (10 μg) were bound to a 1-mL chelating fast flow column and equilibrated with 5 volumes of buffer B (20 mM MES, pH 6.5, 10 mM $CaCl_2$, 10 mM $MgCl_2$, 0.5 M mannitol, and 0.03% β-DM) before removing the extrinsic poteins with 3 volumes of buffer B supplemented with 1 M $CaCl_2$. After washing the column with 5 volumes of buffer B, matrix-bound PSII complexes were incubated with a 10-fold molar excess of the three native extrinsic proteins (PsbO, PsbU, and PsbV) and allowed 30 min for reconstitution. Unbound proteins were then removed by washing with 5 volumes of buffer B, followed by the elution of the PSII complexes. PSII dissection experiments were performed in a similar way (i.e., column-bound PSII was washed with various reagents followed by SDS-PAGE analysis of the eluted PSII).

Mass Spectrometry

MALDI analysis for intact protein subunits was performed on a qTOF mass spectrometer (QSTAR XL; Applied Biosystems). A mixture of five polypeptides (Calibration Mixture 2, Sequazyme peptide mass standards kit; Applied Biosystems) was used for external calibration. PSII preparations (adjusted to 1 mg/mL Chl) were mixed with a saturated solution of 2,5-dihydroxybenzoic acid at a ratio of 2 to 5, and ~1 μL of the analyte mixture was then loaded onto the MALDI plate. Intact mass tags of photosynthetic proteins were determined in the *m/z* range of 3 to 30 kD with a mass accuracy of ~100 ppm at 13.5 kD. MALDI-MS spectra shown are the sum of 1200 to 2400 laser shots at a pulse rate of 20 Hz. For the lipase treatment, PSII samples (10 μg Chl) were incubated with 0.1 units of Lipolase (Novozymes) prior to analysis. Intact PSII subunits were analyzed in the high mass range (30 to 50 kD) using an UltraFlex2.0 MALDI-TOF mass spectrometer (Bruker Daltonics). PSII preparations (adjusted to 1 mg/mL Chl) were mixed with a saturated solution of sinapinic acid at a ratio of 2 to 5, and ~1 μL of the analyte mixture was then loaded onto the MALDI plate.

For the MALDI peptide mass fingerprint analysis of the D1 subunit, protein bands were excised from the polyacrylamide gel and destained with two to three changes of 50% (v/v) acetonitrile buffered with 25 mM NH_4HCO_3. After the gel slices had been completely dried in a vacuum concentrator, they were rehydrated in trypsin solution (12.5 ng/μL trypsin and 25 mM NH_4HCO_3). Enzymatic hydrolyzation was performed overnight at 37°C. Peptide fragments were eluted from the gel matrix by application of 1 volume of elution solution (50% [v/v] acetonitrile and 0.5% [v/v] TFA) and sonication in a water bath for 20 min. The supernatant was spotted on an AnchorChip (Bruker Daltonics) according to the manufacturer's instructions using α-cyano-4-hydroxycynamic acid as the MALDI matrix. MALDI-TOF-MS analysis of tryptic peptides was performed using the UltraFlex2.0 mass spectrometer according to the manufacturer's instructions. The UltraFlex2.0 was equipped with a Scout MTP MALDI target. The spectra were acquired in a mass range from *m/z* 400 to *m/z* 3500 in the positive mode with a target voltage of 25 kV and a pulsed ion extraction of 21.85 kV. The laser frequency was set to 50 Hz, and the spectra shown were a sum of 200 to 400 laser shots. The reflector voltage was set to 26.4 kV and detector voltage to 1.7 kV. For external calibration of the instrument, a peptide standard with *m/z* of 757.399, 1296.684, 1619.822, and 2093.086 D was used. The relative amount of newly synthesized protein after the ^{15}N pulse was calculated according to Gustavsson et al. (2005).

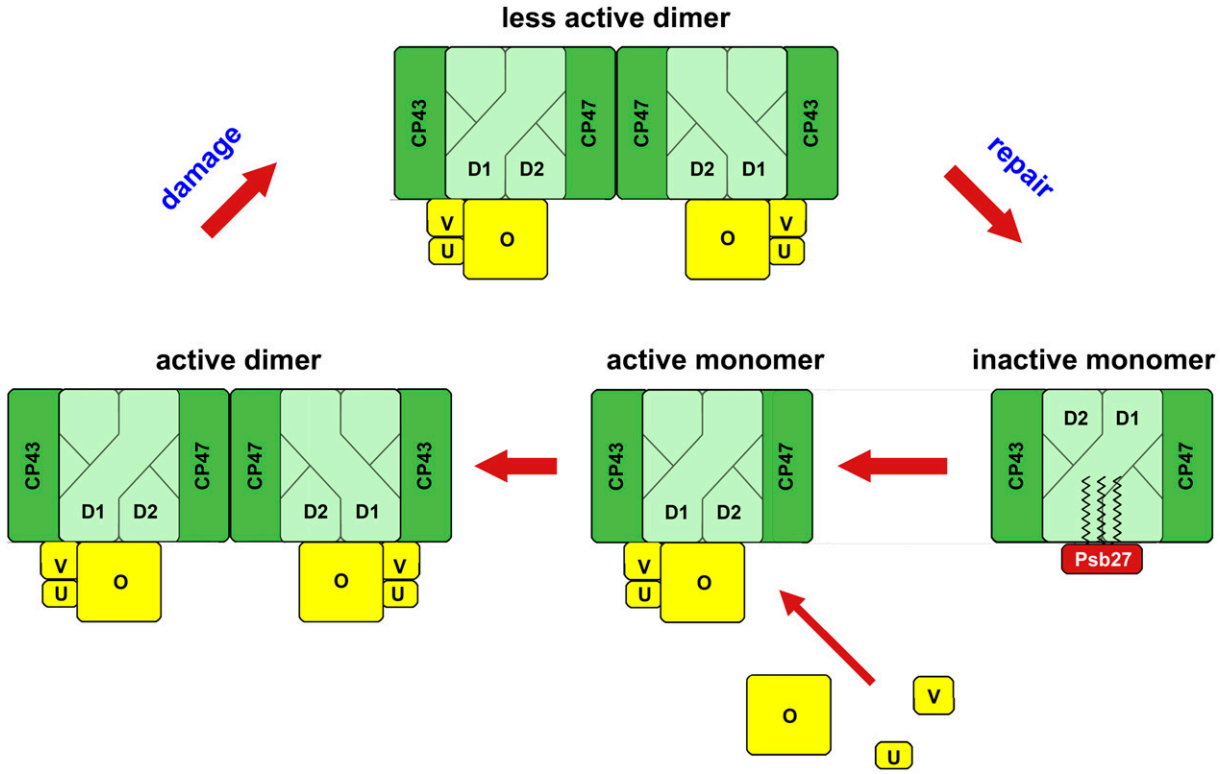

Figure 10. Schematic Model for the Transient PSII Subcomplexes Isolated in This Study.

Upon damage by light, the highly active dimeric PSII complex [$PSII_{D(high)}$] is transformed into a subfraction of less-active PSII [$PSII_{D(low)}$]. In the next step, the D1 subunit and others are exchanged before the inactive monomeric PSII-Psb27 complex [$PSII_{M(low)}$] could be isolated. This complex, which performs light-induced charge separation but is incapable of water splitting as it lacks subunits PsbO, PsbU, and PsbV, is turned into the active PSII monomer [$PSII_{M(high)}$] after release of Psb27 and assembly of the water-splitting site. Finally, two active monomers merge to a highly active dimeric PSII complex [$PSII_{D(high)}$].

Transient Absorption Spectroscopy

Flash-induced absorbance difference spectra of $P680^+Q_A^-$- $P680Q_A$ were measured at low temperature (77K) using a laboratory-built flash spectrophotometer as previously described (Hillmann et al., 1995). PSII complexes were diluted to about 10 μM Chl in 20 mM MES/NaOH, pH 6.5, 10 mM $CaCl_2$, 20 mM KCl, 0.02% β-DM, 2 mM ferrycyanide, and 65% glycerol. The sample was cooled to 77K in a liquid nitrogen bath cryostat (DN 1704; Oxford). The cryostat was centered in the measuring beam of the spectrophotometer. The samples were then excited by saturating flashes of about 15-μs duration from a Xe flash lamp filtered by colored glass (CS96-4; Corning). Measuring light from a 200-W tungsten halogen lamp was passed through a monochromator (spectral bandwidth of 3 nm), the sample, and a combination of interference and edge filters in front of a photomultiplier (EMI 9558BQ) coupled to a transient recorder (Tektronix TDS540). Difference spectra were obtained from the initial amplitude of the flash-induced absorbance changes as a function of the wavelength.

Determination of the Mn Content

The Mn content was determined by electron paramagnetic resonance as free Mn^{2+} before and after extraction of Mn from the PSII complexes by NH_2OH treatment at room temperature. The signal of the $[Mn(H_2O)^6]^{2+}$ complex was recorded with a Bruker EXP300E spectrometer using a microwave frequency of 9.57 GHz. The Mn^{2+} content was estimated from the area under the signal. For calibration, a Mn^{2+} standard solution (Fluka) was used.

Accession Numbers

Sequence data from this article can be found in the National Center for Biotechnology Information protein data library under accession numbers NP_683253 (Psb27), NP_682633 (D1), NP_682420 (D2), NP_682421 (CP43), NP_682320 (CP47), NP_682331 (PsbE), NP_441782 (Psb27; *Synechocystis* sp PCC 6803), NP_897863 (*Synechococcus* WH8102), YP_399362 (*Synechococcus elongatus* PCC7942), YP_321097 (*Anabaena variabilis*), ZP_00107253 (*Nostoc punctiforme* PCC73102), ZP_00514356 (*Crocosphaera watsonii* WH8501), and YP_721473 (*Trichodesmium erythraeum*).

ACKNOWLEDGMENTS

We thank the German Research Council (Sonderforschungsbereich 480, project C1 to M.R. and Sonderforschungsbereich 498, project A6 to E.S.) for financial support and the Protein Center of the Ruhr-University Bochum for infrastructural support. We also thank K.-E. Jaeger and

T. Eggert for advising us on the lipase assay, F. Lendzian for the electron paramagnetic resonance measurements, A. Trebst, S. Oeljeklaus, and J. Nickelsen for stimulating discussions, and M. Çetin, C. König, and R. Oworah-Nkruma for excellent technical assistance.

Received March 21, 2006; revised September 17, 2006; accepted October 27, 2006; published November 17, 2006.

REFERENCES

Anbudurai, P.R., Mor, T.S., Ohad, I., Shestakov, S.V., and Pakrasi, H.B. (1994). The ctpA gene encodes the C-terminal processing protease for the D1 protein of the photosystem II reaction center complex. Proc. Natl. Acad. Sci. USA **91,** 8082–8086.

Anderson, J.M., Park, Y.I., and Chow, W.S. (1997). Photoinactivation and photoprotection of photosystem II in nature. Physiol. Plant **100,** 214–223.

Aro, E.M., Suorsa, M., Rokka, A., Allahverdiyeva, Y., Paakkarinen, V., Saleem, A., Battchikova, N., and Rintamaki, E. (2005). Dynamics of photosystem II: A proteomic approach to thylakoid protein complexes. J. Exp. Bot. **56,** 347–356.

Bendtsen, J.D., Nielsen, H., von Heijne, G., and Brunak, S. (2004). Improved prediction of signal peptides: SignalP 3.0. J. Mol. Biol. **340,** 783–795.

Chen, H., Zhang, D., Guo, J., Wu, H., Jin, M., Lu, Q., Lu, C., and Zhang, L. (2006). A Psb27 homologue in *Arabidopsis thaliana* is required for efficient repair of photodamaged photosystem II. Plant Mol. Biol. **61,** 567–575.

Diner, B.A., and Rappaport, F. (2002). Structure, dynamics, and energetics of the primary photochemistry of photosystem II of oxygenic photosynthesis. Annu. Rev. Plant Biol. **53,** 551–580.

Diner, B.A., Schlodder, E., Nixon, P.J., Coleman, W.J., Rappaport, F., Lavergne, J., Vermaas, W.F., and Chisholm, D.A. (2001). Site-directed mutations at D1-His198 and D2-His197 of photosystem II in Synechocystis PCC 6803: Sites of primary charge separation and cation and triplet stabilization. Biochemistry **40,** 9265–9281.

Ferreira, K.N., Iverson, T.M., Maghlaoui, K., Barber, J., and Iwata, S. (2004). Architecture of the photosynthetic oxygen-evolving center. Science **303,** 1831–1838.

Fyfe, P.K., Hughes, A.V., Heathcote, P., and Jones, M.R. (2005). Proteins, chlorophylls and lipids: X-ray analysis of a three-way relationship. Trends Plant Sci. **10,** 275–282.

Gomez, S.M., Bil, K.Y., Aguilera, R., Nishio, J.N., Faull, K.F., and Whitelegge, J.P. (2003). Transit peptide cleavage sites of integral thylakoid membrane proteins. Mol. Cell. Proteomics **2,** 1068–1085.

Gomez, S.M., Nishio, J.N., Faull, K.F., and Whitelegge, J.P. (2002). The chloroplast grana proteome defined by intact mass measurements from liquid chromatography mass spectrometry. Mol. Cell. Proteomics **1,** 46–59.

Gustavsson, N., Greber, B., Kreitler, T., Himmelbauer, H., Lehrach, H., and Gobom, J. (2005). A proteomic method for the analysis of changes in protein concentrations in response to systemic perturbations using metabolic incorporation of stable isotopes and mass spectrometry. Proteomics **5,** 3563–3570.

Hillmann, B., Brettel, K., van Mieghem, F., Kamlowski, A., Rutherford, A.W., and Schlodder, E. (1995). Charge recombination reactions in photosystem II. 2. Transient absorbance difference spectra and their temperature dependence. Biochemistry **34,** 4814–4827.

Juncker, A.S., Willenbrock, H., Von Heijne, G., Brunak, S., Nielsen, H., and Krogh, A. (2003). Prediction of lipoprotein signal peptides in Gram-negative bacteria. Protein Sci. **12,** 1652–1662.

Kamata, T., Hiramoto, H., Morita, N., Shen, J.R., Mann, N.H., and Yamamoto, Y. (2005). Quality control of photosystem II: An FtsH protease plays an essential role in the turnover of the reaction center D1 protein in Synechocystis PCC 6803 under heat stress as well as light stress conditions. Photochem. Photobiol. Sci. **4,** 983–990.

Kamiya, N., and Shen, J.R. (2003). Crystal structure of oxygen-evolving photosystem II from *Thermosynechococcus vulcanus* at 3.7-A resolution. Proc. Natl. Acad. Sci. USA **100,** 98–103.

Kashino, Y., Lauber, W.M., Carroll, J.A., Wang, Q., Whitmarsh, J., Satoh, K., and Pakrasi, H.B. (2002). Proteomic analysis of a highly active photosystem II preparation from the cyanobacterium Synechocystis sp. PCC 6803 reveals the presence of novel polypeptides. Biochemistry **41,** 8004–8012.

Keren, N., Liberton, M., and Pakrasi, H.B. (2005). Photochemical competence of assembled photosystem II core complex in cyanobacterial plasma membrane. J. Biol. Chem. **280,** 6548–6553.

Klinkert, B., Ossenbuhl, F., Sikorski, M., Berry, S., Eichacker, L., and Nickelsen, J. (2004). PratA, a periplasmic tetratricopeptide repeat protein involved in biogenesis of photosystem II in Synechocystis sp. PCC 6803. J. Biol. Chem. **279,** 44639–44644.

Komenda, J., Barker, M., Kuvikova, S., de Vries, R., Mullineaux, C.W., Tichy, M., and Nixon, P.J. (2006). The FtsH protease slr0228 is important for quality control of photosystem II in the thylakoid membrane of Synechocystis sp. PCC 6803. J. Biol. Chem. **281,** 1145–1151.

Komenda, J., Reisinger, V., Muller, B.C., Dobakova, M., Granvogl, B., and Eichacker, L.A. (2004). Accumulation of the D2 protein is a key regulatory step for assembly of the photosystem II reaction center complex in Synechocystis PCC 6803. J. Biol. Chem. **279,** 48620–48629.

Krogh, A., Larsson, B., von Heijne, G., and Sonnhammer, E.L. (2001). Predicting transmembrane protein topology with a hidden Markov model: Application to complete genomes. J. Mol. Biol. **305,** 567–580.

Kuhl, H., Kruip, J., Seidler, A., Krieger-Liszkay, A., Bunker, M., Bald, D., Scheidig, A.J., and Rogner, M. (2000). Towards structural determination of the water-splitting enzyme. Purification, crystallization, and preliminary crystallographic studies of photosystem II from a thermophilic cyanobacterium. J. Biol. Chem. **275,** 20652–20659.

Loll, B., Kern, J., Saenger, W., Zouni, A., and Biesiadka, J. (2005). Towards complete cofactor arrangement in the 3.0 Å resolution structure of photosystem II. Nature **438,** 1040–1044.

Madan Babu, M., and Sankaran, K. (2002). DOLOP—Database of bacterial lipoproteins. Bioinformatics **18,** 641–643.

Mattoo, A.K., and Edelman, M. (1987). Intramembrane translocation and posttranslational palmitoylation of the chloroplast 32-kDa herbicide-binding protein. Proc. Natl. Acad. Sci. USA **84,** 1497–1501.

Michel, K.P., Thole, H.H., and Pistorius, E.K. (1996). IdiA, a 34 kDa protein in the cyanobacteria Synechococcus sp. strains PCC 6301 and PCC 7942, is required for growth under iron and manganese limitations. Microbiology **142,** 2635–2645.

Nixon, P.J., Barker, M., Boehm, M., de Vries, R., and Komenda, J. (2005). FtsH-mediated repair of the photosystem II complex in response to light stress. J. Exp. Bot. **56,** 357–363.

Ono, T., and Inoue, Y. (1983). Mn-preserving extraction of 33-, 24- and 16-kDa proteins from O2-evolving PS II particles by divalent salt-washing. FEBS Lett. **164,** 255–260.

Peltier, J.B., Emanuelsson, O., Kalume, D.E., Ytterberg, J., Friso, G., Rudella, A., Liberles, D.A., Soderberg, L., Roepstorff, P., von Heijne, G., and van Wijk, K.J. (2002). Central functions of the lumenal and peripheral thylakoid proteome of Arabidopsis determined by experimentation and genome-wide prediction. Plant Cell **14,** 211–236.

Peter, G.F., and Thornber, J.P. (1991). Biochemical composition and organization of higher plant photosystem II light-harvesting pigment-proteins. J. Biol. Chem. **266,** 16745–16754.

Plucken, H., Muller, B., Grohmann, D., Westhoff, P., and Eichacker, L.A. (2002). The HCF136 protein is essential for assembly of the photosystem II reaction center in *Arabidopsis thaliana.* FEBS Lett. **532,** 85–90.

Roose, J.L., and Pakrasi, H.B. (2004). Evidence that D1 processing is required for manganese binding and extrinsic protein assembly into photosystem II. J. Biol. Chem. **279,** 45417–45422.

Rutherford, A.W., and Boussac, A. (2004). Biochemistry. Water photolysis in biology. Science **303,** 1782–1784.

Schagger, H., and von Jagow, G. (1987). Tricine-sodium dodecyl sulfate-polyacrylamide gel electrophoresis for the separation of proteins in the range from 1 to 100 kDa. Anal. Biochem. **166,** 368–379.

Seidler, A. (1996). The extrinsic polypeptides of photosystem II. Biochim. Biophys. Acta **1277,** 35–60.

Shi, L.X., and Schroder, W.P. (2004). The low molecular mass subunits of the photosynthetic supracomplex, photosystem II. Biochim. Biophys. Acta **1608,** 75–96.

Summerfield, T.C., Shand, J.A., Bentley, F.K., and Eaton-Rye, J.J. (2005b). PsbQ (Sll1638) in Synechocystis sp. PCC 6803 is required for photosystem II activity in specific mutants and in nutrient-limiting conditions. Biochemistry **44,** 805–815.

Summerfield, T.C., Winter, R.T., and Eaton-Rye, J.J. (2005a). Investigation of a requirement for the PsbP-like protein in Synechocystis sp. PCC 6803. Photosynth. Res. **84,** 263–268.

Thornton, L.E., Ohkawa, H., Roose, J.L., Kashino, Y., Keren, N., and Pakrasi, H.B. (2004). Homologs of plant PsbP and PsbQ proteins are necessary for regulation of photosystem ii activity in the cyanobacterium Synechocystis 6803. Plant Cell **16,** 2164–2175.

Whitelegge, J.P., Gomez, S.M., Stevens, R.L., Mastrogiacomo, A., Gundersen, C., and Faull, K.F. (1997). Electrospray-ionization mass spectrometry of lipidated intrinsic membrane proteins. FASEB J. **11,** A1088.

Whitelegge, J.P., Gundersen, C.B., and Faull, K.F. (1998). Electrospray-ionization mass spectrometry of intact intrinsic membrane proteins. Protein Sci. **7,** 1423–1430.

Yamamoto, Y., and Ke, B. (1981). Membrane-surface electric properties of triton-fractionated spinach subchloroplast fragments. Biochim. Biophys. Acta **636,** 175–184.

Zak, E., Norling, B., Maitra, R., Huang, F., Andersson, B., and Pakrasi, H.B. (2001). The initial steps of biogenesis of cyanobacterial photosystems occur in plasma membranes. Proc. Natl. Acad. Sci. USA **98,** 13443–13448.

Zouni, A., Witt, H.T., Kern, J., Fromme, P., Krauss, N., Saenger, W., and Orth, P. (2001). Crystal structure of photosystem II from *Synechococcus elongatus* at 3.8 Å resolution. Nature **409,** 739–743.